

Article

# Resilience Regulation Strategy for Container Port Supply Chain under Disruptive Events

Bowei Xu <sup>1,\*</sup> , Weiting Liu <sup>1</sup> and Junjun Li <sup>2,\*</sup>

<sup>1</sup> Institute of Logistics Science & Engineering, Shanghai Maritime University, Shanghai 201306, China

<sup>2</sup> Merchant Marine College, Shanghai Maritime University, Shanghai 201306, China

\* Correspondence: bwxu@shmtu.edu.cn (B.X.); lij@shmtu.edu.cn (J.L.)

**Abstract:** There are many inevitable disruptive events, such as the COVID-19 pandemic, natural disasters and geopolitical conflicts, during the operation of the container port supply chain (CPSC). These events bring ship delays, port congestion and turnover inefficiency. In order to enhance the resilience of the CPSC, a modified two-stage CPSC system containing a container pretreatment system (CPS) and a container handling system (CHS) is built. A two-dimensional resilience index is designed to measure its affordability and recovery. An adaptive fuzzy double-feedback adjustment (AFDA) strategy is proposed to mitigate the disruptive effects and regulate its dynamicity. The AFDA strategy consists of the first-level fuzzy logic control system and the second-level adaptive fuzzy adjustment system. Simulations show the AFDA strategy outperforms the original system, PID, and two pipelines for improved dynamic response and augmented resilience. This study effectively supports the operations manager in determining the proper control policies and resilience management with respect to indeterminate container waiting delay and allocation delay due to disruptive effects.

**Keywords:** modified two-stage container port supply chain; disruptive effects; two-dimensional resilience index; adaptive fuzzy double-feedback adjustment strategy



**Citation:** Xu, B.; Liu, W.; Li, J. Resilience Regulation Strategy for Container Port Supply Chain under Disruptive Events. *J. Mar. Sci. Eng.* **2023**, *11*, 732. <https://doi.org/10.3390/jmse11040732>

Academic Editor: Mihalis Goliass

Received: 12 March 2023

Accepted: 22 March 2023

Published: 28 March 2023



**Copyright:** © 2023 by the authors. Licensee MDPI, Basel, Switzerland. This article is an open access article distributed under the terms and conditions of the Creative Commons Attribution (CC BY) license (<https://creativecommons.org/licenses/by/4.0/>).

## 1. Introduction

The container port supply chain (CPSC) refers to the chain structure which takes the container port as the core and integrates all kinds of service providers (liner companies, train companies, warehousing companies, etc.) and customers (trade companies) into a coordinated entity, so as to achieve the goal of stable operation, higher efficiency and lower cost. Different from the general manufacturing supply chain, the container port supply chain does not create new commodity entities, but adds value by providing services [1]. In the context of the global supply chain, container ports have become important nodes connecting global production, international trade and related logistics activities. According to the current development characteristics of container ports, in addition to the basic function of logistics, it is also an important service and production provider. Therefore, whether container ports operate stably and efficiently affects the interests of many participants in the CPSC, and it has become an indispensable part of the international trade system. Figure 1 shows a basic structure of the container port supply chain.

Under the influence of various disruptive events, container ports tend to be affected by various adverse restrictions, which are mainly manifested as the decrease in port productivity leading to the difficult relief of port operating pressure, the decrease in ship and container turnover efficiency, the shortage of effective transport capacity supply, and the sharp rise of container liner freight rates. Generally, the reduced efficiency of container operation and continuous congestion have become global problems. Hence, the stable, efficient and flexible operation of the CPSC under adverse influences has always been a concern of the country and related stakeholders in the industry, which is a problem worthy of in-depth study.

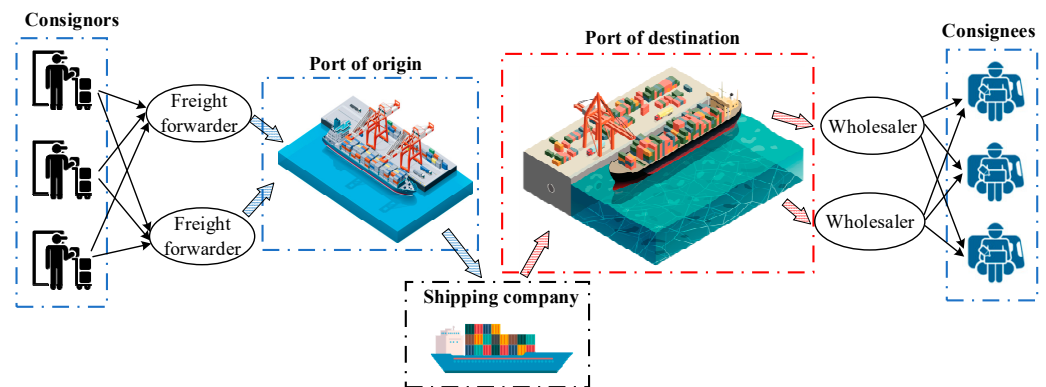


**Figure 1.** Basic structure of container port supply chain.

Control theory has been proved to be a very effective method [2]. It can be used as an effective decision-making tool that helps managers to efficiently control inventory levels throughout the SC, reducing the remarkable percentage of logistics costs [3]. Also, it provides sufficient mathematical tools (such as Laplace transform, Z transform, transfer function and block diagram etc.) to analyze and simulate the systems based on dynamic models [4]. Now, there is an increasing need for effective and efficient production control systems, which have become an important system in the field of industrial engineering. Compared with the classical research methods in the supply chain field, such as operations research and game theory, the main advantage of the control theory method is that it combines the supply chain operation process with the control process, making it convenient to explore the relationships among the internal states and control the production process. In addition, control theory can predict the response to any given input [5], thus having important implications for supply chain systems to operate at desired levels. At present, in the related fields of ports and the shipping supply chain [6–10], existing research mainly focuses on benefit assessment, risk management, and low-carbon operations. Resilience plays an important role in the process of SC operation. It promotes the recovery of the SC under disruptive events [11,12]. Resilience measure guides the optimization and adjustment of the SC [13]. However, the definition of resilience is not uniform [14]. However, the production control modeling of the CPSC and the corresponding regulation strategies are still very limited.

This study constructs a modified two-stage CPSC system. A novel two-dimensional resilience index  $R$  including affordability and recovery is proposed. An adaptive fuzzy double-feedback control is designed to mitigate the disruptive effects. The body of this paper is organized as follows. Section 2 reviews the relevant literature. Section 3 describes the modified two-stage CPSC system in detail. Section 4 explains the two-dimensional resilience index. Section 5 presents the design of the AFDA strategy. Section 6 describes the simulations and the analysis. Finally, the managerial findings and conclusions are drawn in Section 7.

## 2. Literature Review

### 2.1. Supply Chain Risks and Dynamics

The risks suffered by the supply chain (SC) tend to be unpredictable and diverse. Many scholars have considered the disruptive influence of the SC under different unfavorable conditions and disruptions, and put forward corresponding measures. Corsini et al. [15] considered the possible impact on the supply chain of two different disruptive events (failure events and changeovers), and the results pointed out that efficient production control policies (measured in terms of operational efficiency) do not necessarily yield the best results when measured in terms of supply chain efficiency. Ivanov et al. [16] proposed a risk analytics framework and explained the concept of digital SC twins. They studied the impact of digitalization and Industry 4.0 on the ripple effect in the SC and combined

the results gained from the two isolated areas. Olivares-Aguila and ElMaraghy [17] presented a system dynamics model to investigate SC behavior due to disruptions, and found that the SC is affected more when the disruptions take place near to the end-echelon or consumption stages.

In terms of the port supply chain, Zhang and Lam [18] developed a system framework to evaluate the economic losses of industrial clusters caused by port interruptions in three different stages, and finally found that the dynamic inventory control strategy used by manufacturers is conducive to reducing the risk of port interruption. Cuong et al. [19] utilized the four-dimensional fractional Lotka–Volterra competition model and nonlinear analysis methods to study relevant port behaviors and port operation decision-making strategies, and they found that the proposed resilience management scheme can ensure an average growth rate of 7.46% in container throughput. Rogerson et al. [20] analyzed a supply chain disruption from flexibility and capacity perspectives, and results showed that various capacity problems (ports, links, container chassis, empty containers) encountered due to port conflicts can be solved by flexible measures such as nodes, modes and fleet flexibility. Bai et al. [21] analyzed temporal and geospatial port congestion status, and proposed a density-based spatial clustering of applications with noise algorithm to analyze the economic implications of congestion for various stakeholders in the system.

For the abnormal behavior caused by different risks, it is necessary to analyze the dynamics of the supply chain and carry out dynamic control. John et al. [22] proposed the APIOBPCS (automatic pipelines, inventory and order-based production control system) to describe the inventory and production control strategy of the supply chain. On this basis, Alkaabneh et al. [23] conducted research to reduce CO<sub>2</sub> emissions of food supply chains. They developed a spatially and temporally disaggregated price equilibrium mathematical model and compared three emission reduction interventions (carbon tax, technology innovation, and land sparing). Papanagnou [24] implemented a stochastic state-space model to capture the dynamics of a new four-echelon closed-loop supply chain model, and introduced an optimization method to study the impact of the Internet of Things on inventory variance and the bullwhip effect. Cuong et al. [25] proposed a fractional-order sliding mode control algorithm based on the adaptive mechanism, which ensured the robust stability of the goods flow in the supply chain network. Alkaabneh et al. [26] developed a dynamic programming model to optimize resource allocation by food banks among the agencies they serve. Khamseh et al. [27] established a general model based on bounded optimal control theory to optimize supply chain recovery and cost. Fu et al. [28] developed a distributed model predictive control approach to handle supply chain operations and achieve effective supply chain management with minimal information exchange and communication. Alkaabneh and Diabat [29] proposed and compared two different algorithms (branch-and-price and a two-stage meta-heuristic) to solve the multi-objective home healthcare delivery problem. The aim is to minimize the service and routing costs while maximizing compatibility of nurses and patients. Yan et al. [30] designed a stabilizing linear feedback controller to stabilize the supply chain mathematical model with a computer aided digital manufacturing process. Based on system dynamics, Xu et al. [31] established a four-dimensional differential equation with chaotic behavior to describe the multi-level supply chain, and combined this with modern control theory to implement a novel fractional-order adaptive sliding mode control algorithm to achieve efficient management of the supply chain.

It can be seen that the research on the dynamic control of supply chains under various disruptive influences mainly focuses on the manufacturing supply chain. The research on the implementation of dynamic regulation strategies in fields related to the CPSC to achieve effective supply chain optimization and management is still insufficient.

## 2.2. Resilience of Supply Chain

At present, enterprises are paying more and more attention to the research on supply chain resilience. Resilience strategy is not only closely related to the operation level of the supply chain, but also affects the implementation of management decisions. Cohen

et al. [32] investigated the gap between the theory and practice of supply chain resilience, and analyzed the relationship between operations, supply-chain characteristics and implemented strategies. Under the COVID-19 pandemic, Moosavi and Hosseini [33] implemented two resiliency strategies of pre-setting additional inventory and backup suppliers, which helped decision makers to plan for response in the event of a pandemic or any prolonged high-intensity disruption. Mao et al. [34] developed two metrics, cumulative performance loss and fast recovery, to measure the resilience of the supply chain network. Also, three main indicators of network resilience, namely node density, node complexity and node criticality were considered by Rajesh [35], who adopted an improved metaheuristic and crazy elitist TLBO algorithm to ensure cost efficiency in resilience design. Chen et al. [36] established the resilience measurement model of the container transportation network in the port hinterland. Rajesh [37] put forward the resilience fuzzy index to measure the level of resilience of enterprises. Ramezankhani et al. [38] proposed a novel dynamic network data envelopment analysis framework to dynamically evaluate the performance of the supply chain from the two perspectives of sustainability and resilience. Zhang et al. [39] proposed a recovery time equivalent (RTE) disruption risk measurement model using value at risk. Furthermore, considering the strategy of improving resilience, Li et al. [40] explored the relationship between network characteristics and supply chain resilience and came to the conclusion that network characteristics can better explain supply chain network resilience than network type and average degree. Gao et al. [41] studied the relationship between risk control and resilience in the process of digital transformation. The risk control system constructed by a Bayesian belief network could improve the resilience of the supply chain from a risk point of view.

The study of supply chain resilience helps explore the internal mechanism of the existing level of supply chain resilience, so as to judge the necessity of supply chain resilience regulation. At present, there is no unified definition and measurement method of system resilience, and the application of resilience in the CPSC field is lacking. Enhanced resiliency of the CPSC under disruptive events is urgently needed.

### 3. Modified Two-Stage CPSC System

Based on the improvement of the traditional production and inventory control model, the container handling system (CHS) is firstly described, including its overall calculation description, and four major strategies that relate to the actual operation processes of container ports. Further, the container pretreatment system (CPS) is designed and coupled with the CHS, thereby the two-stage CPSC system is established. By selecting appropriate state variables, the state space of the modified two-stage CPSC can reveal the real-time state and dynamic characteristics of each stage of the CPSC system, which is conducive to the analysis of each state in the CPSC system and the formulation of reasonable regulation strategies. Finally, the dynamic characteristics are analyzed and calculated, and the calculation results can be obtained through the relevant theorem. Simulations verify the correctness of the analysis process.

#### 3.1. Container Handling System

The definitions of variables and symbols involved in this paper are shown in Table 1.

The container handling system is shown in Figure 2. Its input is the  $ACHR$  obtained in the previous stage; correspondingly, the unfinished container handling requirement ( $UCHR$ ) is its output. The CHS mainly consists of four processes, i.e., (1) container handling forecasting mechanism, (2) container handling strategy, (3)  $CHIP$  adjustment strategy, and (4)  $UCHR$  adjustment strategy. In CHS, the most important calculation process is that the  $PCHR$  is equal to the average container handling requirement ( $AVCHR$ ) plus the adjustment of unfinished container handling requirement ( $UCHR_{adj}$ ), and the adjustment of container handling in process ( $CHIP_{adj}$ ). Specifically, there are three feedforward links in the CHS. The  $AVCHR$  is obtained by the first-order forecasting link defined by the smoothing constant  $T_A$ , and  $AVCHR$  can obtain  $PCHR$ . Simultaneously,  $AVCHR$  reacts with  $T_Q$  to obtain the

*ECHIP* level, and reacts with  $T_H$  to obtain the *EFCHR*.  $T_P$  represents the delay in the particular container handling process.  $T_{CHIP}$  and  $T_{UCHR}$  are used as the error adjustment time, adjusting the error between *ECHIP* and *CHIP* and the error between *EFCHR* and *UCHR*, respectively.

**Table 1.** Definitions of variables and symbols in this paper.

<i>ACHR</i>	Actual container handling requirement
<i>AVCHR</i>	Average container handling requirement
<i>AVRATE</i>	Actual container average arrive rate
<i>CARATE</i>	Container arrive rate
<i>CHIP</i>	Container handling in progress
<i>CHIP<sub>adj</sub></i>	<i>CHIP</i> adjustment
<i>COMRATE</i>	Handling completion rate
<i>COMRATE<sub>1</sub></i>	Gross allocation completion rate
<i>COMRATE<sub>2</sub></i>	Net allocation completion rate
<i>ECHIP</i>	Expected container handling in progress
<i>ECOM</i>	Expected allocation completion rate
<i>EFCHR</i>	Expected finished container pretreatment requirement
<i>EFCHR</i>	Expected finished container handling requirement
<i>FCPR</i>	Finished container pretreatment requirement
<i>FCPR<sub>adj</sub></i>	<i>FCPR</i> adjustment
<i>OSC</i>	Oscillation level
<i>PCHR</i>	Planned container handling requirement
<i>R</i>	Resilience index
$T_A$	Forecasting smoothing constant
$T_{CHIP}$	Time to adjust <i>CHIP</i> discrepancy
$T_E$	Expected lead-time of pretreatment
$T_{FCPR}$	Time to adjust <i>FCPR</i> discrepancy
$T_H$	Expected handling time
$t_p$	Peak time
$T_P$	Container handling delay time
$T_{P1}$	Allocation time delay
$T_Q$	Expected lead-time of container handling
$t_s$	Setting time
$T_{UCHR}$	Adjustment time of <i>UCHR</i>
$T_{WAIT}$	Waiting time delay
$U_A$	Unit allocation rate
<i>UCHR</i>	Unfinished container handling requirement
<i>UCHR<sub>adj</sub></i>	<i>UCHR</i> adjustment

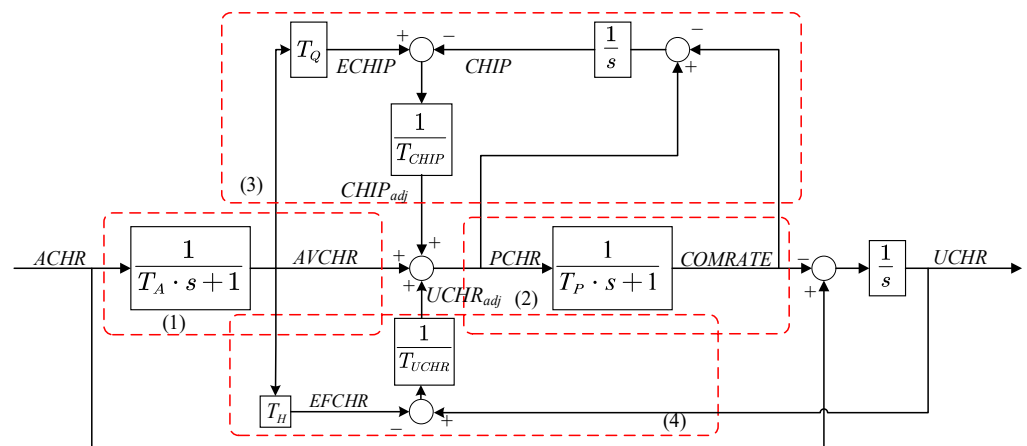


**Figure 2.** Container handling system.

### 3.2. Container Pretreatment System

In CHS, the demand signal  $ACHR$  is generally directly used as its input. However, under disruptive events, the input signal often has to experience a certain delay. At this point, the port productivity receives the signal of container handling requirement in the state of continuous dynamic saturation. Therefore, this paper presents the design of the pretreatment stage, considering the impact of the uncertain container waiting time and berth allocation delay on the input container handling requirement signal. The pretreatment completion rate is used as the input of the next stage. The container pretreatment system (CPS) is shown in Figure 3.

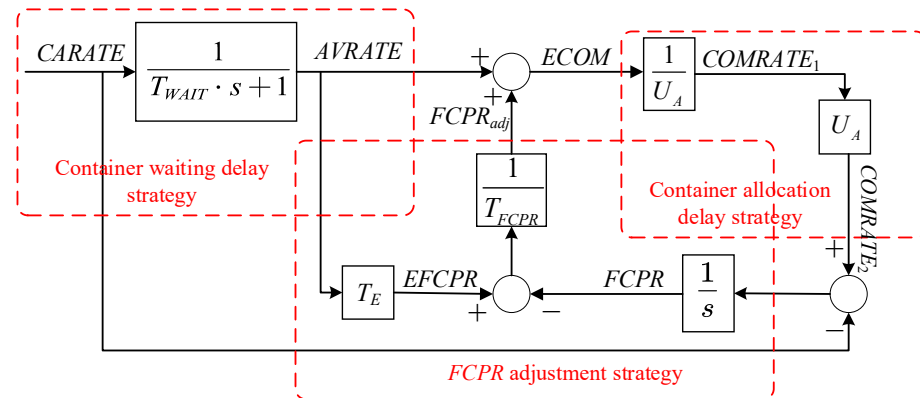


Figure 3. Container pretreatment system.

In the CPS, there are three strategies, namely, the container waiting delay strategy,  $FCPR$  adjustment strategy, and container allocation delay strategy.  $T_{WAIT}$  represents the container waiting time constant. After the effect of the first-order delay set by  $T_{WAIT}$ , the average container arrive rate ( $AVRATE$ ) can be estimated from the actual container arrive rate ( $CARATE$ ). The estimated value from  $CARATE$  ( $AVRATE$ ) can further set the expected  $FCPR$  ( $EFCPR$ ), where  $T_E$  is the expected lead-time of the pretreatment system. The adjustment of  $FCPR$  ( $FCPR_{adj}$ ) can be obtained by the difference between the expected  $FCPR$  and the  $FCPR$  after the adjustment time  $T_{FCPR}$ , and  $T_{FCPR}$  can be used as a proportional control. The sum of the average container arrive rate ( $AVRATE$ ) and the  $FCPR$  adjustment is taken as the expected allocation completion rate ( $ECOM$ ).  $U_A$  represents the unit allocation rate, and the gross allocation completion rate ( $COMRATE_1$ ) can be obtained by the  $ECOM$ . The  $FCPR$  is derived from the difference between the net allocation completion rate ( $COMRATE_2$ ) and the  $CARATE$ .

### 3.3. Two-Stage Container Port Supply Chain System

Figure 4 shows that the two systems (CPS and CHS) take  $COMRATE_1$  ( $ACHR$ ) as the system coupling point to construct the two-stage container port supply chain system. Based on the elaboration of the system in Sections 3.1 and 3.2, the specific formula description of the two-stage container port supply chain system can be obtained. For the CPS, the only input is the  $CARATE$ , and the output  $COMRATE_1$  is taken as the input of the next stage. The  $CARATE$  can be deduced as

$$ECOM(t) = FCPR_{adj}(t) + AVRATE(t) \tag{1}$$

where

$$FCPR_{adj}(t) = \frac{1}{T_{FCPR}} \cdot [AVRATE(t) \cdot T_E - FCPR(t)] \tag{2}$$

and



### 3.4. State Space Description

The state-space approach provides a complete system description. Using the state space description can clearly explore the dynamics of each state in the two-stage CPSC system, and it is also the premise of effectively analyzing and verifying the dynamic characteristics. Furthermore, state dynamics can also provide an important reference for resilience regulation strategies. In the two-stage CPSC system, due to the existence of first-order lags, it is not easy to analyze the internal connection relationships and select appropriate state variables. Hence, it is necessary to modify the two-stage CPSC to make it more in line with the requirements of state space analysis. The first-order lag can be considered as integral and time constant [43]. The modified two-stage CPSC system is shown in Figure 5.

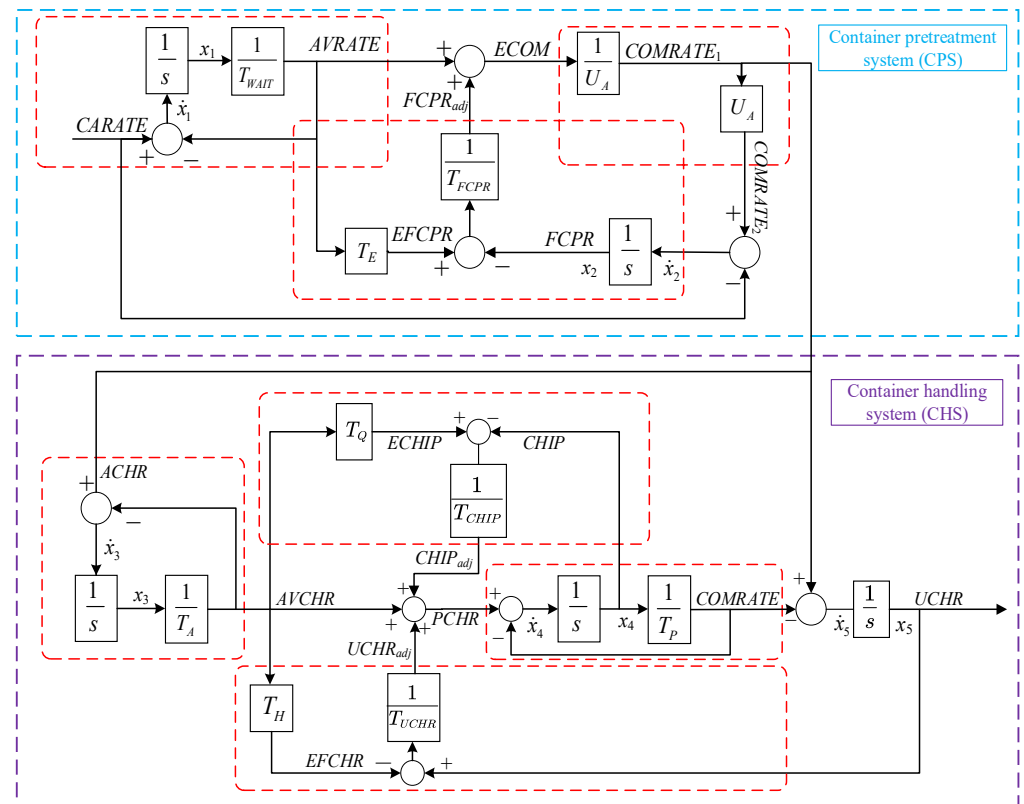


Figure 5. Modified two-stage container port supply chain system.

The state variable can be effectively selected according to the integral links in the block diagram. For the container pretreatment system (CPS),  $AVRATE \cdot T_{WAIT} = x_1$ ,  $FCPR = x_2$ .  $x_1$  reflects the status of the actual container arrive rate, and  $x_2$  indicates the status of the FCPR. Furthermore, the derivative state of each state variable can be obtained as follows:

$$\dot{x}_1 = -\frac{1}{T_{WAIT}}x_1 + CARATE \tag{9}$$

$$\dot{x}_2 = U_A \cdot COMRATE_1 - CARATE \tag{10}$$

Considering  $COMRATE_1 = ACHR$ , Equation (10) can be rewritten as

$$\dot{x}_2 = U_A \cdot ACHR - CARATE \tag{11}$$

In addition, *ECOM* is also a state that should be noted, which can be expressed as

$$\begin{aligned} ECOM &= FCPR_{adj} + AVRATE \\ &= \frac{1}{T_{WAIT}}x_1 + \frac{1}{T_{FCPR}}\left(\frac{T_E}{T_{WAIT}}x_1 - x_2\right) \\ &= \left(\frac{1}{T_{WAIT}} + \frac{T_E}{T_{WAIT}T_{FCPR}}\right)x_1 - \frac{1}{T_{FCPR}}x_2 \end{aligned} \tag{12}$$

Similarly, for the container handling system (CHS), the state variables can also be reasonably selected according to the corresponding principles as follows:

$$AVCHR \cdot T_A = x_3 \tag{13}$$

$$CHIP = x_4 \tag{14}$$

$$UCHR = x_5 \tag{15}$$

Therefore, the derivative state of  $x_1, x_2,$  and  $x_3$  can be obtained as

$$\dot{x}_3 = -\frac{1}{T_A}x_3 + ACHR \tag{16}$$

$$\dot{x}_5 = \left(\frac{1}{T_A} + \frac{T_Q}{T_{CHIP}T_A} - \frac{T_H}{T_{UCHR}T_A}\right)x_3 - \left(\frac{1}{T_p} + \frac{1}{T_{CHIP}}\right)x_4 + \frac{1}{T_{UCHR}}x_5 \tag{17}$$

$$\dot{x}_5 = -\frac{1}{T_p}x_4 + ACHR \tag{18}$$

As the key calculation process in the CHS, the state of *PCHR* can be obtained as

$$\begin{aligned} PCHR &= CHIP_{adj} + AVCHR + UCHR_{adj} \\ &= \left(\frac{1}{T_A} + \frac{T_Q}{T_{CHIP}T_A} - \frac{T_H}{T_{UCHR}T_A}\right)x_3 - \frac{1}{T_{CHIP}}x_4 + \frac{1}{T_{UCHR}}x_5 \end{aligned} \tag{19}$$

The continuous closed-loop state space of the modified two-stage CPSC system can be expressed as

$$\dot{x} = \begin{bmatrix} A & 0 \\ 0 & B \end{bmatrix} x + \begin{bmatrix} 1 \\ -1 \\ 0 \\ 0 \\ 0 \end{bmatrix} CARATE + \begin{bmatrix} 0 \\ U_A \\ 1 \\ 0 \\ 1 \end{bmatrix} ACHR \tag{20}$$

where

$$A = \begin{bmatrix} -\frac{1}{T_{WAIT}} & 0 \\ 0 & 0 \end{bmatrix}, B = \begin{bmatrix} -\frac{1}{T_A} & 0 & 0 \\ \frac{1}{T_A} + \frac{T_Q}{T_{CHIP}T_A} - \frac{T_H}{T_{UCHR}T_A} & -\frac{1}{T_p} - \frac{1}{T_{CHIP}} & \frac{1}{T_{UCHR}} \\ 0 & -\frac{1}{T_p} & 0 \end{bmatrix} \tag{21}$$

At the same time, the internal states of the modified two-stage CPSC system can also be expressed as

$$\begin{bmatrix} ECOM \\ COMRATE_1 \\ PCHR \\ UCHR \end{bmatrix} = \begin{bmatrix} C & 0 \\ 0 & D \end{bmatrix} x \tag{22}$$

where

$$C = \begin{bmatrix} \frac{1}{U_A} + \frac{T_E}{T_{WAIT}T_{FCPR}} & -\frac{1}{T_{FCPR}} \\ \frac{1}{U_A} \left( \frac{1}{T_{WAIT}} + \frac{T_E}{T_{WAIT}T_{FCPR}} \right) & -\frac{1}{T_{FCPR}U_A} \end{bmatrix}, D = \begin{bmatrix} \frac{1}{T_A} + \frac{T_Q}{T_{CHIP}T_A} - \frac{T_H}{T_{UCHR}T_A} & -\frac{1}{T_{CHIP}} & \frac{1}{T_{UCHR}} \\ 0 & 0 & 1 \end{bmatrix} \quad (23)$$

### 3.5. Dynamic Characteristic Analysis

In order to further obtain the relevant insights on the dynamic characteristics of the modified two-stage CPSC system, it is necessary to use the transfer function and the corresponding characteristic equation for analysis. Based on the state-space description, the main transfer functions in CPS and CHS can be obtained as

$$\frac{COMRATE_1}{CARATE} = \frac{1}{U_A} \cdot \frac{(T_{FCPR} + T_{WAIT} + T_E)s + 1}{T_{FCPR}T_{WAIT} s^2 + (T_{FCPR} + T_{WAIT})s + 1} \quad (24)$$

$$\frac{ECOM}{CARATE} = \frac{(T_{FCPR} + T_{WAIT} + T_E)s + 1}{T_{FCPR}T_{WAIT} s^2 + (T_{FCPR} + T_{WAIT})s + 1} \quad (25)$$

$$\frac{UCHR}{ACHR} = \frac{T_A T_P T_{CHIP} s^2 + (T_P T_{CHIP} + T_A T_{CHIP} + T_A T_P)s + T_P - T_Q + T_H T_{CHIP} / T_{CHIP}}{T_{CHIP} T_P T_A [1 / T_{UCHR} T_P + (1 / T_{CHIP} + 1 / T_P)s + s^2] (s + 1 / T_A)} \quad (26)$$

$$\frac{PCHR}{ACHR} = \frac{s^2 (T_{CHIP} T_P T_{UCHR} + T_P T_{UCHR} T_Q - T_P T_{CHIP} T_H + T_P T_A T_{CHIP}) + s (T_{UCHR} T_{CHIP} + T_{UCHR} T_Q - T_H T_{CHIP} + T_P T_{CHIP} + T_A T_{CHIP}) + T_{CHIP}}{T_{UCHR} T_{CHIP} T_P T_A [1 / T_{UCHR} T_P + (1 / T_{CHIP} + 1 / T_P)s + s^2] (s + 1 / T_A)} \quad (27)$$

Based on the obtained transfer functions Equations (24)–(27), the final steady-state value can be obtained by using the final value theorem, and it is beneficial to compare with the subsequent simulation to verify the correctness of the results. When the system input is set as a unit step signal, it is easy to obtain the relevant final values:

$$\begin{aligned} \lim_{s \rightarrow 0} \cdot \frac{COMRATE_1}{CARATE} &= \frac{1}{U_A}, \quad \lim_{s \rightarrow 0} \cdot \frac{ECOM}{CARATE} = 1 \\ \lim_{s \rightarrow 0} \cdot \frac{UCHR}{ACHR} &= \frac{T_{UCHR}(T_P - T_Q)}{T_{CHIP}} + T_H, \quad \lim_{s \rightarrow 0} \cdot \frac{PCHR}{ACHR} = 1 \end{aligned} \quad (28)$$

Further, for the modified two-stage CPSC system, the corresponding final values are

$$\lim_{s \rightarrow 0} \cdot \frac{UCHR}{CARATE} = \lim_{s \rightarrow 0} \cdot \frac{COMRATE_1}{CARATE} \cdot \frac{UCHR}{ACHR} = \frac{1}{U_A} \left[ \frac{T_{UCHR}(T_P - T_Q)}{T_{CHIP}} + T_H \right] \quad (29)$$

$$\lim_{s \rightarrow 0} \cdot \frac{PCHR}{CARATE} = \lim_{s \rightarrow 0} \cdot \frac{COMRATE_1}{CARATE} \cdot \frac{PCHR}{ACHR} = \frac{1}{U_A} \quad (30)$$

As expected, the result of each final value is similar to the conclusion drawn by Xu et al. [44], which proves that the calculation is correct and reasonable. It can be seen that the value of  $uchr(\infty)$  depends on  $U_A, T_{UCHR}, T_{CHIP}, T_P, T_Q$  and  $T_H$ . When  $T_P = T_Q, U_A = 1$  and  $T_H = 0, uchr(\infty) = 0$ .

In addition, the dynamic performance is usually determined by the characteristic equation in the transfer function. The standard form of the characteristic equation of the second-order CPS is

$$s^2 + 2\zeta\omega_n s + \omega_n^2 = 0 \quad (31)$$

where  $\omega_n$  and  $\zeta$  represent the natural frequency and damping ratio, respectively.  $\omega_n$  is related to the recovery speed of its response to reach a steady state, while  $\zeta$  determines the oscillation level of its response. Compared with Equations (24) and (25), we have

$$\omega_n = \sqrt{\frac{1}{T_{WAIT}T_{FCPR}}} \quad (32)$$

$$\begin{aligned} \zeta &= \frac{(T_{WAIT} + T_{FCPR})}{2} \sqrt{\frac{1}{T_{WAIT} T_{FCPR}}} \\ &= \frac{1}{2} \sqrt{2 + \frac{T_{WAIT}^2 + T_{FCPR}^2}{T_{WAIT} T_{FCPR}}} \end{aligned} \tag{33}$$

As can be seen from Equations (32) and (33), both  $\omega_n$  and  $\zeta$  depend on  $T_{WAIT}$  and  $T_{FCPR}$ . When the values of  $T_{WAIT}$  and  $T_{FCPR}$  increase,  $\omega_n$  decreases accordingly, causing the response to take longer to return to the steady state. For  $\zeta$ , since both a and b are positive, it is easy to obtain  $T_{WAIT}^2 + T_{FCPR}^2 \geq 2T_{WAIT}T_{FCPR}$ , thus making  $\zeta \geq 1$ . The system is always in a critically damped or overdamped state, which means that the CPS can maintain the stability under any positive control parameters.

For the CHS, since the third-order system has more control parameters, it is not easy to perform an analysis. Therefore, using the characteristic equation to analyze the CHS is an effective choice. The characteristic equation is expressed as

$$\left[1/T_{UCHR} T_P + (1/T_{CHIP} + 1/T_P)s + s^2\right](s + 1/T_A) \tag{34}$$

Setting the three poles obtained by the characteristic equation as  $p, p_1,$  and  $p_2$ , it is easy to identify one of the poles as  $p = -1/T_A$ . Then,

$$p_1 + p_2 = \frac{1}{T_{CHIP}} + \frac{1}{T_P}, \quad p_1 p_2 = \frac{1}{T_{UCHR} T_P} \tag{35}$$

As all relevant control parameters are positive in this paper, it can be obtained that  $p_1 + p_2 > 0, p_1 p_2 > 0,$  and  $1/T_A > 0$ . Therefore, the CHS also maintains stability.

Finally, the classic unit step signal is used as input to simulate each state and initially verify the correctness of the above calculation and analysis. Now, set  $T_P = T_Q, T_H = 1, T_{CHIP} = 2T_P$ . On the premise that  $T_{WAIT}$  is taken as the main independent variable, the states involved are shown in Figure 6.

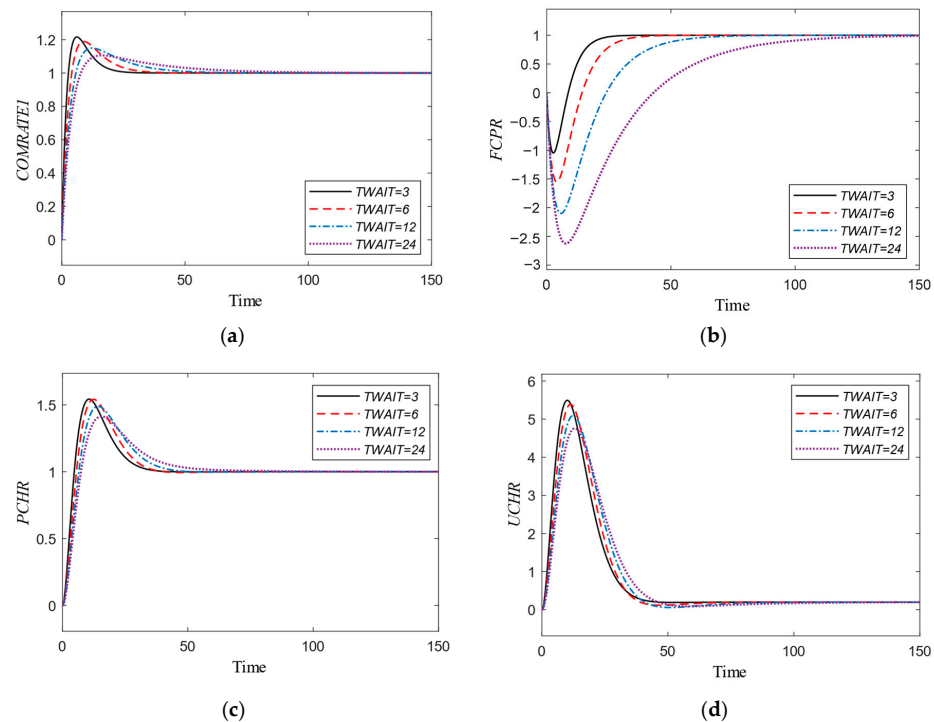


**Figure 6.** Changes of each state in the CPS with different control parameters. (a)  $COMRATE_1$  under the change of  $T_{WAIT}$ ; (b)  $FCPR$  under the change of  $T_{WAIT}$ ; (c)  $PCHR$  under the change of  $T_{WAIT}$ ; (d)  $UCHR$  under the change of  $T_{WAIT}$ .

As shown in Figure 6,  $COMRATE_1$ ,  $PCHR$ , and  $UCHR$  show an initial rise, while the  $FCPR$  shows a rapid initial drop. The reason lies in the transient response caused by the mutated input unit step signal to the responses. Under the influence of the increasing  $T_{WAIT}$ , the setting time of each response increases correspondingly, at the cost of the decreasing oscillation level in varying degrees. The simulation results preliminarily prove the correctness of the calculation and analysis.

#### 4. Two-Dimensional Resilience Index

In the existing literature, the research on the resilience measurement for the supply chain control model is still very insufficient, among which the  $ITAE$  has been proved to be an effective reference for the measurement of the resilience level [44,45]. The  $ITAE$  can effectively reflect the accumulation of the error between the actual unsatisfied container handling requirement and the ideal value over time. If the response fails to reach the steady state or there is a persistent steady-state error, the value of the  $ITAE$  tends to be infinite, indicating that the supply chain is seriously lacking resilience. Based on the equal measurement of positive error and negative error, the smaller the value of the  $ITAE$ , the smaller the deviation between the measured value and the desired value, meaning the better the resilience. The basic calculation of  $ITAE$  can be expressed as

$$ITAE = \int_0^{\infty} t \cdot |e(t)| dt = \lim_{\delta t \rightarrow 0} \sum_{t=0}^{\infty} t |e(t)| \delta t \tag{36}$$

where  $e(t)$  represents the error between actual value and desired value.

However, for the modified two-stage CPSC system, the  $ITAE$  with a single response error is not enough to fully measure its resilience, which may lead to inaccurate results. Therefore, on the basis of the  $ITAE$ , this paper further incorporates the fluctuation degree ( $FL$ ) of the planned container handling requirement ( $PCHR$ ) relative to the container arrive rate ( $CARATE$ ), which is based on the related calculation idea of the bullwhip effect, as shown in Equation (37).

$$\text{Bullwhip} = \frac{\sigma_{ORATE}^2}{\sigma_{CONS}^2} \tag{37}$$

where  $\sigma_{ORATE}^2$  and  $\sigma_{CONS}^2$  refer to the order rate variance and consumption variance in the production and inventory control system. Regarding this criterion, if  $\sigma_{ORATE}^2 / \sigma_{CONS}^2 = 1$ , there is zero bullwhip in the system; if  $\sigma_{ORATE}^2 / \sigma_{CONS}^2 > 1$ , the system is amplified; if  $\sigma_{ORATE}^2 / \sigma_{CONS}^2 < 1$ , the system is smoothed [46]. Therefore, the calculation idea of the bullwhip effect is integrated into the resilience design of the modified two-stage CPSC system. The calculation form is rewritten as Equation (38), so as to reflect the fluctuation of its internal states.  $FL$  is expressed as

$$FL = \left[ \int_0^{\infty} (PCHR(t))^2 dt / \int_0^{\infty} (CARATE(t))^2 dt \right] \tag{38}$$

Now, based on comprehensive consideration of the error level and internal state of the CPS and CHS, the two-dimensional resilience index  $R$  including recovery and affordability is proposed. The resilience index  $R$  is expressed as

$$R = \sqrt{FL^2 + RE^2} \tag{39}$$

where

$$FL = \left[ \int_0^{\infty} (PCHR(t))^2 dt / \int_0^{\infty} (CARATE(t))^2 dt \right], \tag{40}$$

$$RE = \sqrt{\alpha [ITAE_{UCHR}]^2 + \beta [ITAE_{FCPR}]^2}$$

and

$$ITAE_{UCHR} = \int_0^{\infty} t|E_{UCHR}|dt, ITAE_{FCPR} = \int_0^{\infty} t|E_{FCPR}|dt \tag{41}$$

In Equations (38) and (39), *FL* characterizes the fluctuation of the *PCHR* relative to its input in the first stage. Smaller fluctuation stands for more accurate response and higher affordability. Different from the calculation of the traditional bullwhip effect, the calculation of *FL* is carried out in the time domain, and can comprehensively consider the state of the current stage and its input from the previous stage. The ratio of the two is used as the fluctuation degree relative to the input, which can fully reflect the affordability under disruptive events. *RE* integrates the deviation of the two stage responses as the deviation of the whole system. Furthermore, *FL* tends to the degree of fluctuation within the system, while *RE* tends to the deviation of responses, which can be represented as the recovery under disruptive events. The designed two-dimensional resilience index can comprehensively measure the recovery and affordability of the system.

In Equation (40), the accumulation of deviations of *UCHR* and *FCPR* over time is expressed by  $ITAE_{UCHR}$  and  $ITAE_{FCPR}$ , respectively. When the values of  $ITAE_{UCHR}$  and  $ITAE_{FCPR}$  are smaller, the response and recovery are better.  $\alpha$  and  $\beta$  are the proportional coefficients, which is to coordinate the order of magnitude of each calculation link. Therefore, for the novel two-dimensional index *R*, smaller *R* represents better resilience. In Equation (41),  $E_{UCHR} = uchr(t) - uchr(\infty)$ ,  $E_{FCPR} = fcpr(t) - fcpr(\infty)$ . Furthermore, it has been obtained from Equation (33) that  $uchr(\infty) = T_{UCHR}(T_P - T_Q) / T_{CHIP}$ ,  $fcpr(\infty) = 1$ .

## 5. Adaptive Fuzzy Double-Feedback Adjustment Strategy

### 5.1. Overall Strategy Design

Previous studies on the optimal control of supply chain systems tend to obtain the optimal parameters or parameter sets to achieve the optimal system performance [47–49]. However, the obtained mathematical optimal value often does not conform to the actual production process. Considering the limitation, this paper puts forward a design for an adaptive fuzzy double-feedback adjustment (AFDA) strategy. The AFDA includes the first-level fuzzy logic control system and the second-level adaptive fuzzy adjustment system. The AFDA can not only make use of its own real-time states for the adaptive adjustment, but also effectively integrate the relevant logic experience of managers to regulate the fuzzy logic.

An adaptive fuzzy double-feedback control structure is established with two feedback links of *FCPR* and *UCHR*.  $T_{WAIT}$  is the main independent variable, while  $T_P$  and  $TP_1$  are intrinsic properties. The first-level fuzzy logic system is used to realize the adaptive optimization of the control parameters  $T_{FCPR}$  and  $T_{UCHR}$ , and the second-level adaptive fuzzy adjustment system is used to synchronously update the adjustment factors in the fuzzy control process to further optimize the modified two-stage CPSC system control effect. The overall design is shown in Figure 7.

Figure 7 shows the deviation between the *FCPR* and *CARATE* ( $e_1$ ), and its change rate ( $ec_1$ ) as the inputs of first-level fuzzy logic subsystem 1. The smoothing coefficient  $\alpha_1$  is regulated by the set fuzzy logic, and the updated *FCPR* obtained by the updated control parameter  $T_{FCPR}$  is fed back to the modified two-stage CPSC system. Meanwhile,  $K_1$  and  $K_2$  are the adjustment factors of the deviation  $e_1$  and deviation change rate  $ec_1$  respectively, and the control ratio of  $e_1$  and  $ec_1$  can be adjusted in real time, so as to better adapt to changes of external environment. The specific fuzzy design of the first-level fuzzy logic system and the second-level adaptive fuzzy adjustment system will be detailed in Sections 5.2 and 5.3. For the first-level fuzzy logic subsystem 2, the principle is roughly similar to that of subsystem 1; the main difference is that it receives the deviation between the unfinished container handling requirement *UCHR* and the *CARATE* ( $e_2$ ) and the change rate of deviation ( $ec_2$ ) as input. The updated  $T_{UCHR}$  is obtained by the smoothing coefficient  $\alpha_2$ . The updated *UCHR* obtained by  $T_{UCHR}$  is fed back to the modified two-stage CPSC

system.  $K_3$  and  $K_4$  also adjust the corresponding control ratio to better optimize their control effect.

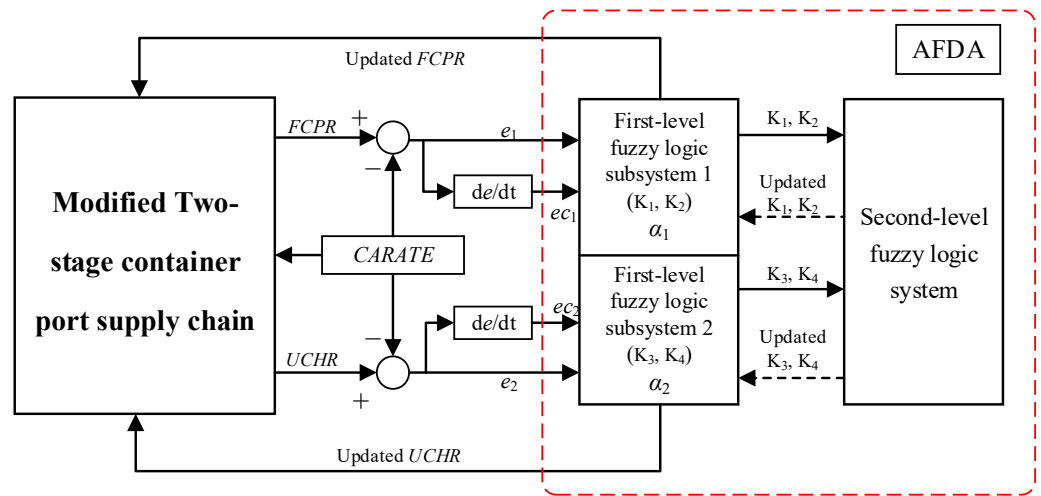


Figure 7. Structure diagram of modified two-stage CPSC system based on AFDA.

5.2. First-Level Fuzzy Logic System

For the first-level fuzzy logic subsystem 1, when the error signal  $e_1$  and the error change rate signal  $ec_1$  between the  $FCPR$  and  $CARATE$  are received,  $T_{FCPR}$  is adjusted by the smoothing coefficient  $\alpha_1$ , and the calculation principle can be expressed as

$$T_{FCPR} = \frac{1 - \alpha_1}{\alpha_1} \tag{42}$$

Since all control parameters are positive,  $\alpha_1 < 1$ . Therefore, the range of the fuzzy output of the first-level fuzzy logic subsystem 1 is defined as  $\{0, 1\}$ . The fuzzy domain of fuzzy inputs is also set as  $\{0, 1\}$ . Further, the number of fuzzy subsets is set as 7, which is a generally applicable setting, i.e.,  $\{VS, S, RS, M, RB, B, VB\}$ . Furthermore, considering that the changes of  $e$  and  $e_1$  are relatively uniform, the membership function which can be set as the uniformly distributed trigonometric functions, has good accuracy and is convenient to calculate. Specific settings can be found in Appendix A. The variation range of the trigonometric membership function is consistent with the domain corresponding to the fuzzy subset.

The fuzzy setting of the first-level fuzzy logic subsystem 2 is similar to that of subsystem 1.  $T_{UCHR}$  is regulated by the smoothing coefficient  $\alpha_2$ . According to the input–output logic relationship, the rule table of fuzzy control of the two fuzzy logic subsystems is shown in Table 2.

Table 2. Rule table of first-level fuzzy logic.

$ec$	$e$						
	VS	S	RS	M	RB	B	VB
VS	M	RS	RS	S	S	VS	VS
S	RB	M	RS	RS	S	S	VS
RS	RB	RB	M	RS	RS	S	S
M	B	RB	RB	M	RS	RS	S
RB	B	B	RB	RB	M	RS	RS
B	VB	B	B	RB	RB	M	RS
VB	VB	VB	B	B	RB	RB	M

Table 2 shows the change trend of the smoothing coefficient ( $\alpha_1, \alpha_2$ ) is consistent with error change rate  $ec$  ( $ec_1, ec_2$ ) and opposite to error ( $e_1, e_2$ ). Therefore, the basic control principle of the first-level fuzzy logic system can be summarized as follows: when the change rate is relatively large, the smoothing coefficient should be increased to alleviate the rapid change of the modified two-stage CPSC system under disruptive events, and when the error is relatively large, it is necessary to reduce the smoothing coefficient to try to restore the error to ideal states.

### 5.3. Second-Level Adaptive Fuzzy Adjustment System

Generally, one of the important characteristics of the modified two-stage CPSC system using fuzzy control is that it is convenient to combine the experience of relevant managers to adjust it. However, because different managers have subjective differences, and the same manager may make different decisions, the parameter design of fuzzy control often has a certain degree of subjectivity. Hence, the real-time adaptive adjustment of the adjustment factors is required.

In the second-level adaptive fuzzy adjustment system, the control objective is to optimize the control effect of the first-level fuzzy logic system through adaptive control of the adjustment factors. The fuzzy subset of the fuzzy inputs is set as {NB, NM, NS, Z, PS, PM, PB}. The membership function also adopts uniformly distributed trigonometric functions. Since the control accuracy of the adjustment factors is often not as high as that of the smoothing coefficient, the number of subsets of the fuzzy output can be selected as 5, i.e., {VS, S, M, B, VB}. It should be noted that at this time, the membership function adopts the trapezoidal membership function with uneven distribution, because the output adjustment factors are mainly distributed at both ends of the interval, and the trapezoidal membership function can smoothly adjust the fuzzy output. The input and output fuzzy domains are {0, 1}. The setting of the fuzzy rule table of the second-level adaptive fuzzy adjustment system is shown in Table 3. More details can be found in Appendix A.

**Table 3.** Fuzzy rule table of second-level adaptive fuzzy adjustment system.

$ec$	$e$						
	NB	NM	NS	Z	PS	PM	PB
NB	B	B	M	VS	S	M	B
NM	B	B	M	S	S	B	B
NS	VB	B	M	M	M	B	VB
Z	VB	B	B	M	B	B	VB
PS	VB	B	M	M	M	B	VB
PM	B	B	M	S	M	B	B
PB	B	M	S	VS	S	M	B

From Table 3, the fuzzy rule presents obvious symmetry characteristics. When both  $e$  and  $ec$  are close to zero (Z), the proportion of the two input adjustment factors of the fuzzy system is equal. When  $e$  becomes larger (positive or negative), the corresponding adjustment factor also becomes larger. This means that it is necessary to increase the control ratio of error and contain it in time. Similarly, when the  $ec$  tends to the extreme value (positive or negative), it is necessary to reduce the control ratio of  $e$  to increase the control ratio of  $ec$ , so as to alleviate the change rate. As a result, the expectation of adaptive adjustment can be achieved.

## 6. Simulations and Analysis

Disruptive events that have negative effects on the CPSC are diverse, such as the repeated spread of the COVID-19 pandemic [50], natural disasters [51] and geopolitical conflicts [52]. Although these disruptive events are different, their impacts on the CPSC can be summarized as demand mutation, uncertain delays, inefficient port productivity, and slow turnover [50–52]. Furthermore, the commonality of these restrictions is that they are

often manifested by the inefficiency, stagnation and congestion of container ports. Therefore, the corresponding constraints are modeled as uncertain container handling waiting time delay and berth allocation delay, thereby exploring their impact on the modified two-stage CPSC and further designing the resilience regulation strategy.

### 6.1. The Effect of CPS on the Modified Two-Stage CPSC

Container uncertain waiting delays and berth allocation delays under disruptive events are integrated into the container preprocessing stage, thereby constructing a CPS. Studying the overall effect of the CPS on the modified two-stage CPSC, especially the change of the main independent variable  $T_{WAIT}$ , can effectively reflect the adverse influences of disruptive events, and the preparations for the follow-up regulation research can be made.

In simulation, the oscillation level and setting time are used to represent the fluctuation degree and stability time, respectively. According to our investigation, the continuation of disruptive events has caused varying congestion or disruption in the CPSC. Specifically, under disruptive events, the specific constraints and the general scheme can be summarized as follows: (1) The impact of the COVID-19 pandemic on the CPSC is strong [50], including extremely high transportation prices, transportation accessibility, and extension of supply chains. (2) The median duration of port disruption caused by natural disasters was 6 days, with 95% of them being 22.2 days [51]. (3) A crisis in the CPSC caused by the conflict between Russia and Ukraine reveals the impact of changes in EU consumer prices in situations of container ports destruction [52]. Combined with the commonality of the investigated supply chains, this paper uses the uncertain container waiting delay and allocation delay links set by the CPS system to explore the impact of disruptive events on the modified two-stage CPSC system.

On this basis, we refer to the real-time data of the most congested container ports in the world, and take the congestion data of the top 20 container ports as an example to calculate the average value of nearly a month. Without losing generality, the system is set to take one day as a cycle. The average waiting time is set to 6 days; the average port handling time is 4 days; the expected pretreatment cycle is 1 day; and the constant  $T_A = 6$  days.  $T_A$  can be given different values according to the specific prediction mechanism, but  $T_A$  does not change the overall response trend of the system to a large extent;  $T_Q$  and  $T_P$  are set to be the same value, that is,  $T_Q = T_P = 4$  days.

Figure 8 shows the effects of  $T_{WAIT}$  on the dynamic behaviors of responses in the CPS. It should be emphasized that, compared with other three performance indicators, it is interesting to see that the *OSC* shows an opposite change trend, because when the waiting time increases, at the cost of longer setting time, the fluctuation becomes less. Furthermore, the responses always experience an initial rise, which is particularly evident in the *UCHR* response. The reason for this is that the mutated step demand is transmitted to the CPSC through the container preprocessing system, and the responses has to satisfy the output signal transmitted by the CPS. Then, with the continuous port productivity, the *UCHR* level is gradually reduced to the required level. Consistent with the analysis in Section 3.4, when  $T_{WAIT}$  increases, the oscillation levels of the *UCHR* and *PCHR* decrease, which are achieved at the expense of longer setting time. In comparison, *CHIP* is less sensitive to the change of  $T_{WAIT}$ . When  $T_{WAIT}$  is small, the oscillation peak of *CHIP* does not change significantly, which proves that when the CPSC is less affected (small  $T_{WAIT}$ ), a certain balance can still be maintained between the port productivity and the planned container handling requirement.

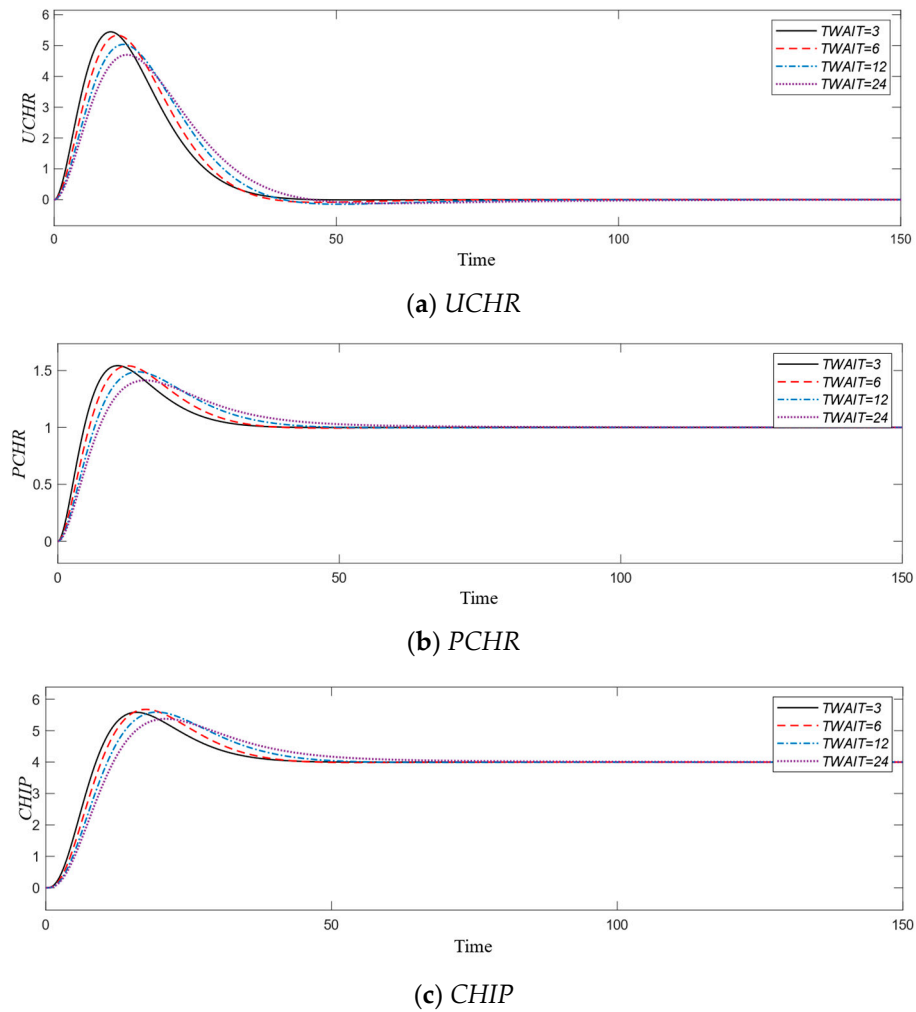


Figure 8. The influence of  $T_{WAIT}$  changes in CPS on responses. (a) UCHR; (b) CHIP; (c) PCHR.

In addition, the modified two-stage CPSC is abbreviated as the original system. The according resilience  $R$  is shown in Figure 9.

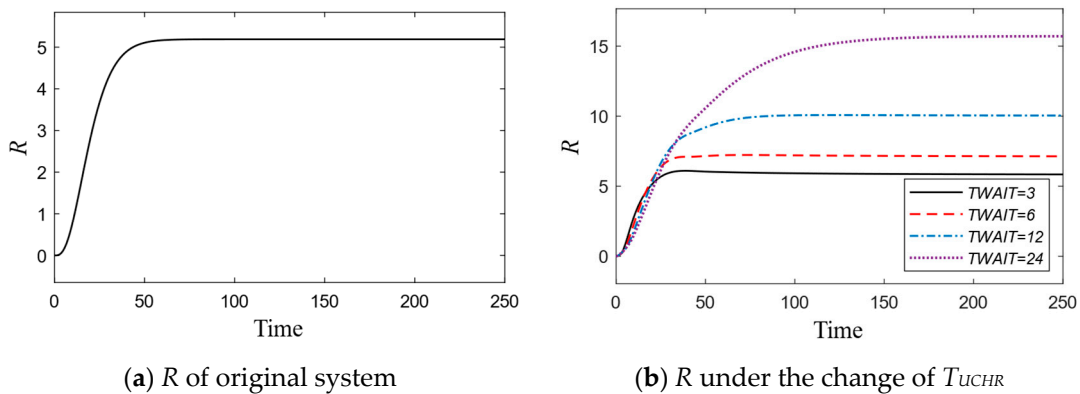


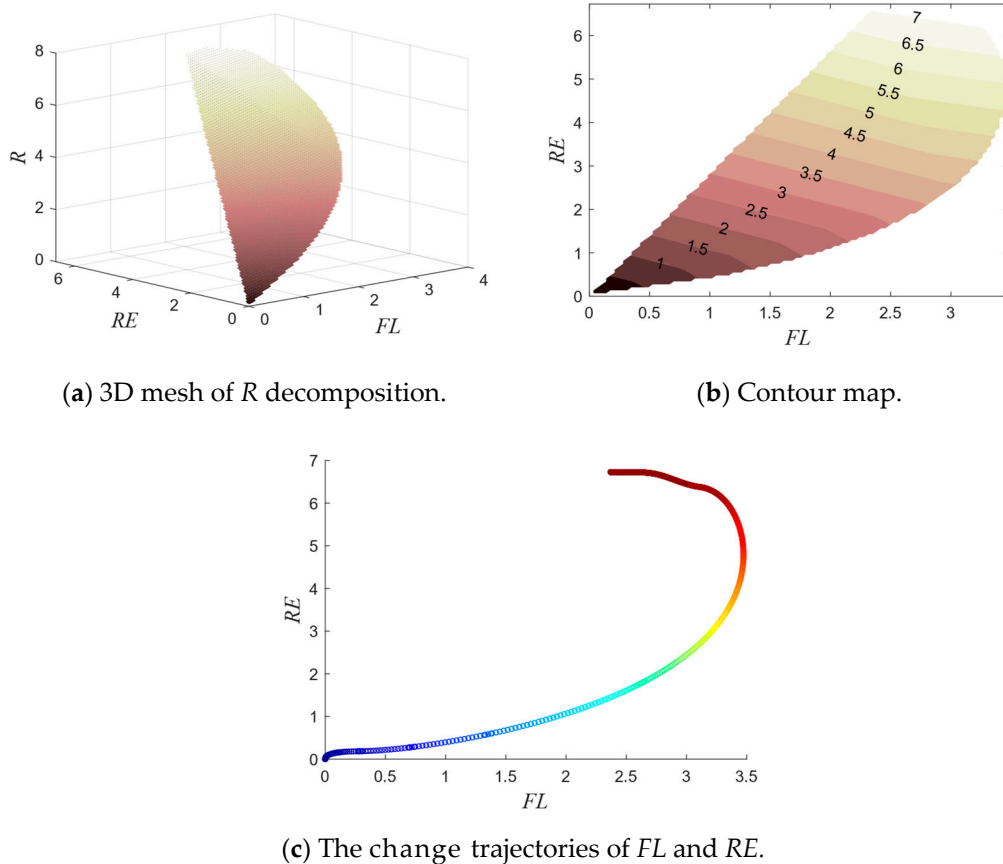
Figure 9. Resilience of original system and the system under the influence of  $T_{WAIT}$ . (a)  $R$  of original system; (b)  $R$  under the change of  $T_{UCHR}$ .

Figure 9b shows that a small  $T_{WAIT}$  can make the resilience response have a faster response speed. When  $T_{WAIT}$  increases, the response speed of  $R$  becomes slower and the final stable value is obviously larger, which means that when the modified two-stage CPSC system is more seriously affected (larger  $T_{WAIT}$ ), the resilience will be significantly reduced.

Compared with the initial system, CPS has weakened the resilience to a certain extent under larger values of  $T_{WAIT}$ , and the resilience is reduced by 66.95% in the worst case.

Based on the derived  $R$ , the effect of  $FL$  and  $RE$  on  $R$  can be further analyzed by decomposing  $R$ .

Figure 10 shows the decomposition of  $R$ , revealing the relationship between the resilience index  $R$  and the internal two-dimensional factors. As shown in Figure 10a,b, both  $RE$  and  $FL$  have a gain effect on  $R$  at the current value, and compared with the affordability, the gain of the recovery to  $R$  is significantly greater than the affordability, which means that the recovery accounts for more weight than the affordability, and the resilience is more affected by the recovery. Figure 10c represents the trajectory of  $RE$  and  $FL$  moving with  $R$  during operation.  $FL$  and  $RE$  eventually move to 2.4 and 6.9, respectively, which is in line with the trend shown by the 3D grid diagram and contour diagram.



**Figure 10.** The 3D mesh, contour map and trajectory of decomposed  $R$ . (a) 3D mesh of decomposition; (b) contour map; and (c) the trajectories of  $FL$  and  $RE$ .

Finally, the relevant specific values in simulations are measured and recorded in Table 4. Further, the weakening degree caused by the CPS is shown in the Table 5.

**Table 4.** Simulation results under the change of parameters.

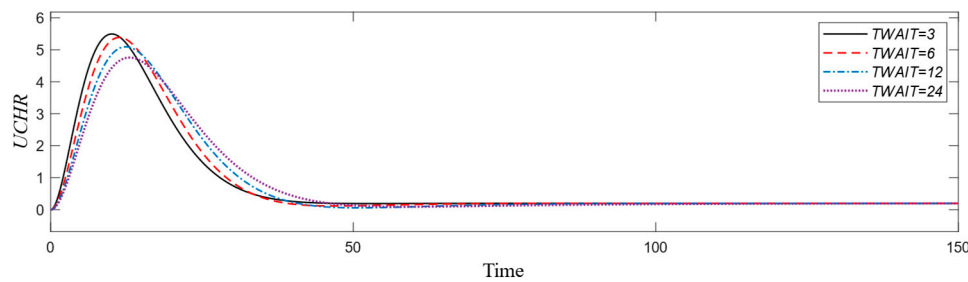
Control Parameters		UCHR			R
		OSC	$t_s$ (d)	$t_p$ (d)	
$T_{FCPR} = 4$	$T_{WAIT} = 3$	5.44	40.60	10.00	5.94
	$T_{WAIT} = 6$	5.33	57.30	11.20	7.24
	$T_{WAIT} = 12$	5.03	72.80	12.30	10.16
	$T_{WAIT} = 24$	4.70	87.10	12.90	15.82
Ideal situation		4.70	36.40	9.10	5.19

**Table 5.** Relative weakening degree of system dynamic performance.

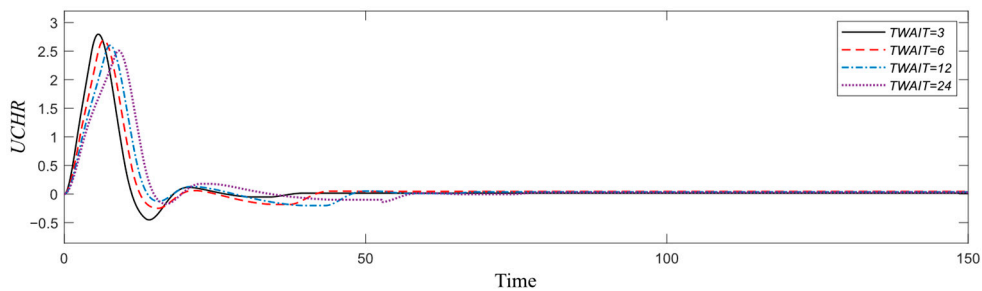
Control Parameters	UCHR			R
	OSC	$t_s$	$t_p$	
$T_{WAIT} = 3$	15.74%	11.54%	9.89%	14.45%
$T_{WAIT} = 6$	13.40%	57.42%	23.08%	39.50%
$T_{WAIT} = 12$	7.02%	100.00%	35.16%	95.76%
$T_{WAIT} = 24$	0	139.29%	41.76%	204.48%

**6.2. Adaptive Fuzzy Double-Feedback Adjustment Strategy for Modified Two-Stage CPSC System**

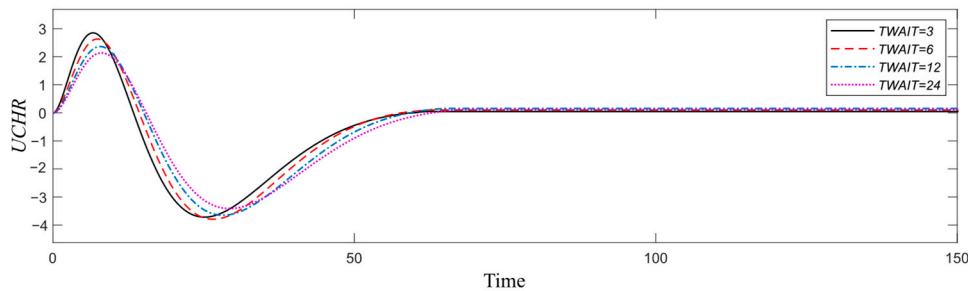
The control objective of the modified two-stage CPSC system is to design appropriate regulation strategies to minimize the negative impact and achieve rapid recovery under disruptive events. An adaptive fuzzy double-feedback control structure is established based on two feedback pipelines. Through the effective control of the smoothing coefficients, the adaptive adjustment of the modified two-stage CPSC system is realized. Similarly, the UCHR is taken as the main control object, and the uncertain waiting time delay is taken as the independent variable. At the same time, the AFDA strategy is compared with the original system, PID, and two pipelines (TP) to verify its effectiveness. The simulation results are shown in Figures 11 and 12.



(a) Original system

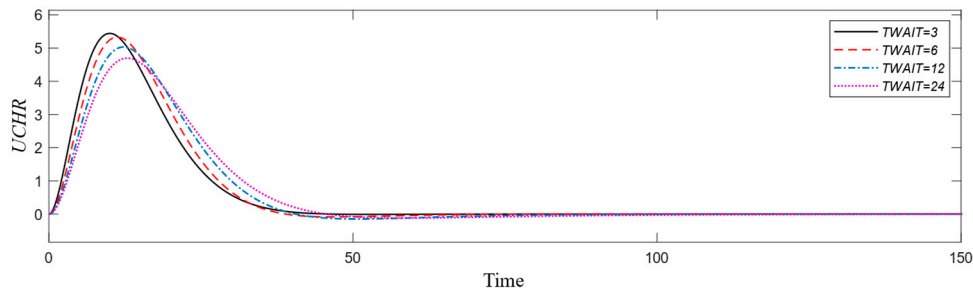


(b) AFDA



(c) PID

**Figure 11.** Cont.



(d) Two pipelines

Figure 11. Comparison of responses: (a) Original system; (b) AFDA; (c) PID; and (d) two pipelines.

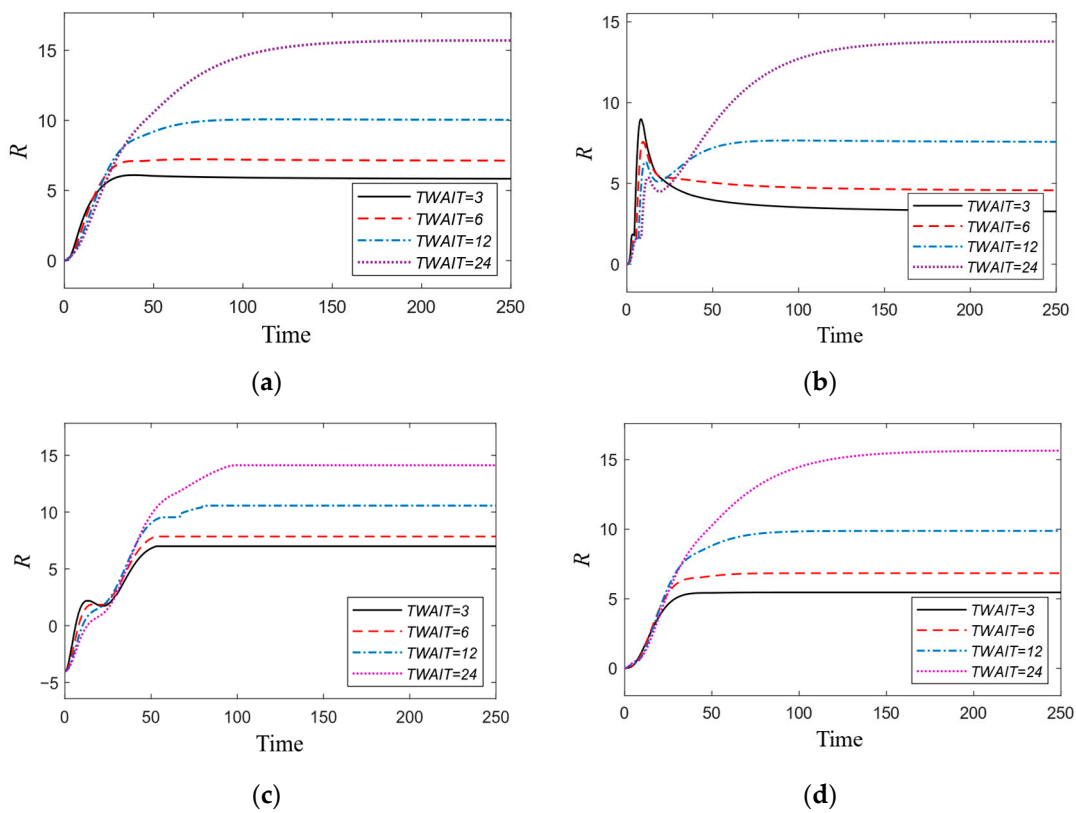


Figure 12. Comparisons of R. (a) Original system; (b) AFDA; (c) PID; and (d) two pipelines.

The simulation results are recorded in Tables 6–8. In Figure 11, the optimization effect of each method can be easily compared and the effectiveness of the proposed AFDA is verified. Compared with the original system, the oscillation level under disruptive effects is significantly reduced, and the stabilization time is shortened. Comparing the data recorded in Table 6 with Table 4, the OSC can be reduced by up to 49.53% at the maximum, and the  $t_s$  can be shortened by up to 35.94%. When the container waiting time delay is (3, 6, 12, 24) days, AFDA can ultimately shorten the stability time by (28.25%, 28.62%, 35.44%, 35.94%), respectively.

**Table 6.** Dynamic performance and  $R$  with AFDA.

	UCHR			$R$
	OSC	$t_s$	$t_p$	
Increase in $T_{WAIT}$	2.80	35.40	5.70	3.27
	2.69	40.90	6.60	4.57
	2.60	47.00	7.60	7.58
	2.51	55.80	9.00	13.78

**Table 7.** Dynamic performance and  $R$  with PID.

	UCHR			$R$
	OSC	$t_s$	$t_p$	
Increase in $T_{WAIT}$	2.86	82.50	6.60	7.58
	2.63	86.50	7.30	8.78
	2.36	94.00	7.80	11.05
	2.14	102.00	8.10	15.40

**Table 8.** Dynamic performance and  $R$  with TP.

	UCHR			$R$
	OSC	$t_s$	$t_p$	
Increase in $T_{WAIT}$	5.44	40.70	10.00	5.87
	5.33	57.30	11.20	6.84
	5.03	72.80	12.30	9.89
	4.70	87.20	12.90	15.64

Figure 12 shows the resilience under different methods. The increase in  $T_{WAIT}$  significantly decreases the resilience. However, using the AFDA strategy, the resilience is enhanced. It is worth noting that  $R$  under the AFDA strategy has an obvious initial rapid rise. The reason is that when the feedback signal is used for adjustment, the initial rise of response affects the measurement of  $R$ . Eventually, both the response and  $R$  can be restored to the stable states.

Finally, for  $R$  with AFDA, it can also be decomposed to further explore the inner two-dimensional mechanism of resilience, as shown in Figure 13.

Figure 13 shows that when  $T_{WAIT}$  is small,  $R$  is significantly affected by  $FL$  more than  $RE$ . This trend begins to change as  $T_{WAIT}$  grows larger. When the value of  $T_{WAIT}$  becomes large,  $R$  is obviously dependent on the change of  $RE$ , while the change of  $FL$  is no longer obvious.

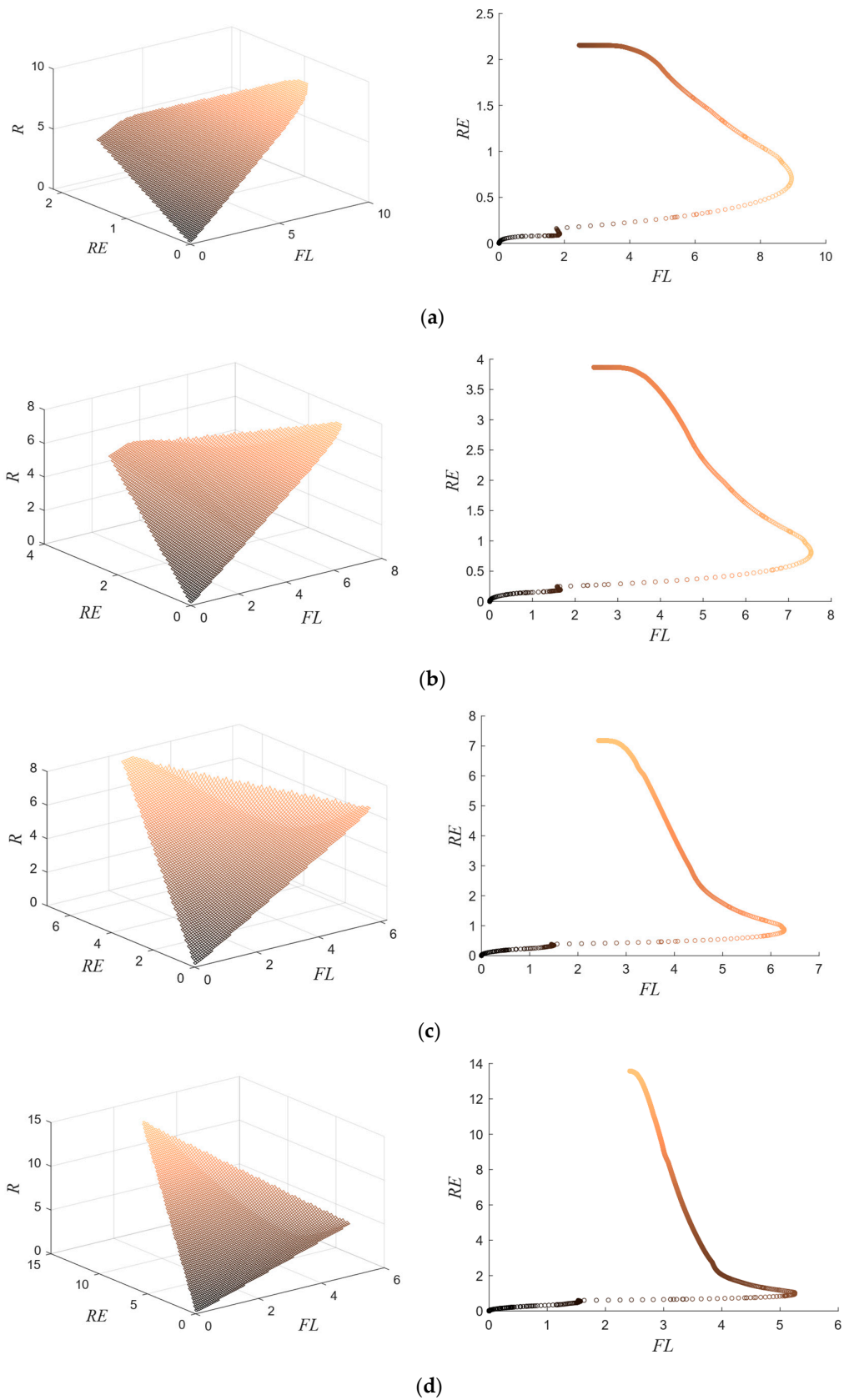


**Figure 13.** The decomposition of  $R$  under AFDA. (a)  $T_{WAIT} = 3$ ; (b)  $T_{WAIT} = 6$ ; (c)  $T_{WAIT} = 12$ ; (d)  $T_{WAIT} = 24$ .

## 7. Managerial Findings and Conclusions

### 7.1. Managerial Findings

Some potentially meaningful managerial findings can be further obtained. (1) Under disruptive events, the efficiency of responses decreases obviously with the extension of waiting time delay. (2)  $R$  is sensitive to the disruptive events. The resilience is greatly weakened under the effect of the CPS. When  $T_{WAIT} = 24$ ,  $T_{FCPR} = 4$ , the resilience can be reduced to as little as 1/3 of that of the original system. (3) Since resilience reflects the inherent property of the CPSC, it is more difficult to measure resilience than other performance indicators. The proposed two-dimensional resilience index can integrate recovery and affordability. Under the same  $T_{WAIT}$ , the resilience can be improved by (44.95%, 36.88%, 25.39%, 12.90%), respectively. (4) When  $T_{WAIT}$  is small,  $R$  is mainly affected by the affordability. When  $T_{WAIT}$  becomes larger, the CPSC needs more recovery, and  $R$  begins to mainly depend on the recovery.

In addition, some management implications and practical suggestions can be proposed. (1) When disruptive events occur, managers in the CPSC can first reasonably model the negative effects and conduct preliminary quantitative analysis, which is more conducive to loss assessment and subsequent adjustment measures. (2) In the actual operation process, the inherent resilience is easy to ignore and difficult to observe directly. Therefore, it is important to consider the guidance for resilience in combination with operations. (3) When managing and optimizing the CPSC, the overall operating logic should be fully considered to avoid local optimization and adjustment. When suffering from disruptive events, the deviation between the container handling requirement and the ideal level is large, and the smoothing coefficient should be properly decreased to try to restore the error to ideal states. While the change rate of error is relatively large, it is necessary to increase the smoothing coefficient to alleviate the rapid change of the CPSC.

### 7.2. Conclusions

A modified two-stage CPSC including CPS and CHS is designed. Indeterminate container waiting delay and allocation delay due to disruptive effects are factored into the CPS. The state-space description and associated characteristic analysis not only provide a comprehensive insight into the CPSC system, but also obtain the theoretical value of the CPSC system response. The two-dimensional resilience index  $R$  includes affordability and recovery. Furthermore, the two-dimensional mechanism of  $RE$  and  $FL$  is explored by decomposing  $R$ . An adaptive fuzzy double-feedback adjustment strategy is designed to realize the adaptive optimization of the CPSC. Compared with other three strategies, the proposed AFDA meets the actual needs of port production practice more easily. When facing different constraints and control objectives, it is easy to change the input and output of fuzzy control and reset the fuzzy logic. Future research will focus on the optimal resilience of the CPSC and the role of various internal factors of resilience.

**Author Contributions:** Conceptualization, B.X. and J.L.; methodology, B.X., J.L. and W.L.; validation, B.X., J.L. and W.L.; writing—review and editing, B.X., J.L. and W.L.; supervision, B.X. and J.L. All authors have read and agreed to the published version of the manuscript.

**Funding:** This work is supported by the National Natural Science Foundation of China (No. 52102466), the Natural Science Foundation of Shanghai (No. 21ZR1426900) and the Soft Science Research Project of Shanghai (No. 22692108100; 23692107400). Here we would like to express our gratitude to them.

**Institutional Review Board Statement:** Not applicable.

**Informed Consent Statement:** Not applicable.

**Data Availability Statement:** The data used to support the findings of this study are included within the article.

**Acknowledgments:** The authors thank the helpful comments and suggestions of anonymous reviewers on this study.

**Conflicts of Interest:** The authors declared no potential conflict of interest with respect to the research, authorship, and/or publication of this article.

### Appendix A

The membership functions in the fuzzification process, the values of the variables involved, and other related fuzzy settings are given in detail. The input and output of the first-level fuzzy logic system and the input of the second-level adaptive fuzzy adjustment system, uniformly distributed trigonometric functions are as follows:

$$f(x, a, b, c) = \begin{cases} \frac{x-a}{b-a} & a \leq x < b \\ \frac{a-c}{b-c} & b \leq x < c \\ 0 & x < a, x \geq c \end{cases} \tag{A1}$$

where  $a, b,$  and  $c$  are the abscissas of three points of the trigonometric membership functions, and  $x$  specifies the domain scope of the variable. The cording value range and coordinate values of each trigonometric function are shown in Table A1.

**Table A1.** The relevant settings of the trigonometric membership functions.

Fuzzy Subsets	Input $x$ ( $e, ec$ )	Abscissas of Trigonometric Function ( $a, b, c$ )
VS	$0 \leq x \leq 5\%$	$(a, b, c) = (0, 0, 0.1667)$
S	$5\% \leq x \leq 16.67\%$	$(a, b, c) = (0, 0.1667, 0.3333)$
RS	$16.67\% \leq x \leq 33.33\%$	$(a, b, c) = (0.1667, 0.3333, 0.5)$
M	$33.33\% \leq x \leq 50\%$	$(a, b, c) = (0.3333, 0.5, 0.6667)$
RB	$50\% \leq x \leq 66.67\%$	$(a, b, c) = (0.5, 0.6667, 0.8333)$
B	$66.67\% \leq x < 83.33\%$	$(a, b, c) = (0.6667, 0.8333, 1)$
VB	$83.33\% \leq x \leq 100\%$	$(a, b, c) = (0.8333, 1, 1)$

The output of the second-level adaptive fuzzy adjustment system adopts the trapezoidal membership functions, and the expression is

$$f(x, a, b, c, d) = \begin{cases} 0, & x < a \\ \frac{x-a}{b-a} & a \leq x \leq b \\ 1 & b < x < c \\ \frac{d-x}{d-c} & c \leq x \leq d \\ 0, & d < x \end{cases} \tag{A2}$$

where  $a, b, c,$  and  $d$  specify the shape of the trapezoidal membership functions, and  $x$  specifies the domain scope of the variable. The specific setting of each membership function is shown in Table A2.

**Table A2.** The relevant settings of the trapezoidal membership functions.

Fuzzy Subsets	Coordinate Range $x$ ( $e, ec$ )	Abscissas of Trapezoidal Function ( $a, b, c, d$ )
VS	$0 \leq x \leq 25\%$	$(a, b, c, d) = (0, 0, 0.05, 0.1)$
S	$25\% \leq x \leq 37.5\%$	$(a, b, c, d) = (0.05, 0.1, 0.15, 0.3)$
M	$37.5\% \leq x \leq 62.5\%$	$(a, b, c, d) = (0.1, 0.2, 0.35, 0.65)$
B	$62.5\% \leq x \leq 75\%$	$(a, b, c, d) = (0.55, 0.8, 0.9, 1)$
VB	$75\% \leq x \leq 100\%$	$(a, b, c, d) = (0.9, 0.95, 1, 1)$

Based on the membership functions of input and output and other related settings, the fuzzy reasoning process adopted is in the form of if-then, shown in Figure A1.

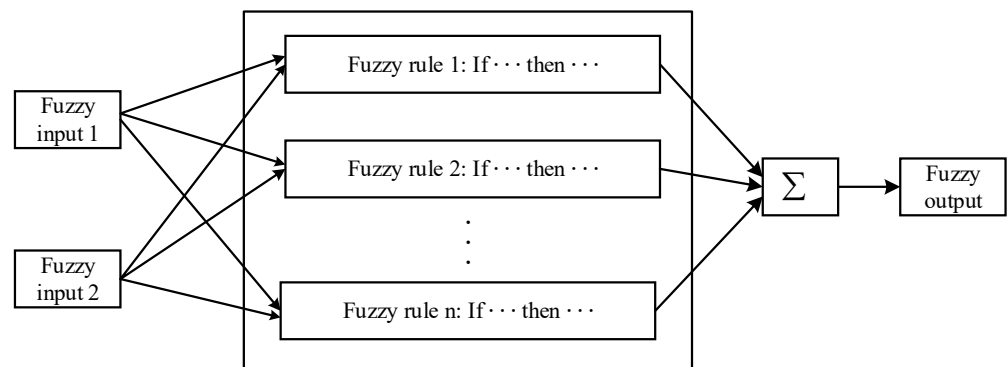


Figure A1. Basic process of fuzzy reasoning.

Finally, the initial settings of the main variables and parameters involved before the fuzzification procedure are shown in Table A3.

Table A3. The initial settings of the main variables and parameters before the fuzzification procedure.

Symbols	Values
$T_{UCHR}$	6
$T_{FCPR}$	4
$\alpha_1$	1/5
$\alpha_2$	1/7
$K_1 = K_2$	0.5
$K_3 = K_4$	0.5

References

- Jiang, B.; Li, J.; Shen, S. Supply chain risk assessment and control of port enterprises: Qingdao port as case study. *Asian J. Shipp. Logist.* **2018**, *34*, 198–208.
- Mason-Jones, R.; Naim, M.M.; Towill, D.R. The impact of pipeline control on supply chain dynamics. *Int. J. Logist. Manag.* **1997**, *8*, 47–62. [CrossRef]
- Sabbaghnia, A.; Razmi, J.; Babazadeh, R.; Moshiri, B. Reducing the Bullwhip effect in a supply chain network by application of optimal control theory. *RAIRO-Oper. Res.* **2018**, *52*, 1377–1396.
- Aggelogiannaki, E.; Sarimveis, H. Design of a novel adaptive inventory control system based on the online identification of lead time. *Int. J. Prod. Econ.* **2008**, *114*, 781–792.
- Sethi, S.P.; Thompson, G.L. *Optimal Control Theory: Applications to Management Science and Economics*; Springer Science & Business Media: Cham, Switzerland, 2018.
- Loh, H.S.; Zhou, Q.; Thai, V.V.; Wong, Y.D.; Yuen, K.F. Fuzzy comprehensive evaluation of port-centric supply chain disruption threats. *Ocean Coast. Manag.* **2017**, *148*, 53–62.
- Ji, H.; Sui, Y.; Wang, H. Sustainable development for shipping companies: A supply chain integration perspective. *J. Coast. Res.* **2017**, *98*, 339–343.
- Liu, F.; Wang, J.; Liu, J.; Kong, Y. Coordination of port service chain with an integrated contract. *Soft Comput.* **2019**, *24*, 6245–6258. [CrossRef]
- Wang, C.; Jiao, Y. Shipping companies’ choice of low sulfur fuel oil with government subsidy and different maritime supply chain power structures. *Marit. Policy Manag.* **2022**, *49*, 323–346.
- Ma, H.L.; Leung, L.C.; Chung, S.H.; Wong, C.W.H. Insurance incentive to shippers by a container port: Issues of risk management in supply chain finance. *Ann. Oper. Res.* **2022**, 1–19. [CrossRef]
- Spieske, A.; Birkel, H. Improving supply chain resilience through industry 4.0: A systematic literature review under the impressions of the COVID-19 pandemic. *Comput. Ind. Eng.* **2021**, *158*, 107452. [PubMed]
- Hohenstein, N.O.; Feisel, E.; Hartmann, E.; Giunipero, L. Research on the phenomenon of supply chain resilience: A systematic review and paths for further investigation. *Int. J. Phys. Distrib. Logist. Manag.* **2015**, *45*, 90–117. [CrossRef]
- Sawik, T. Stochastic optimization of supply chain resilience under ripple effect: A COVID-19 pandemic related study. *Omega* **2022**, *109*, 102596. [CrossRef]
- Negri, M.; Cagno, E.; Colicchia, C.; Sarkis, J. Integrating sustainability and resilience in the supply chain: A systematic literature review and a research agenda. *Bus. Strategy Environ.* **2021**, *30*, 2858–2886. [CrossRef]

15. Corsini, R.R.; Costa, A.; Cannella, S.; Framinan, J.M. Analysing the impact of production control policies on the dynamics of a two-product supply chain with capacity constraints. *Int. J. Prod. Res.* **2022**, *61*, 1913–1937. [[CrossRef](#)]
16. Ivanov, D.; Dolgui, A.; Das, A.; Sokolov, B. Digital supply chain twins: Managing the ripple effect, resilience, and disruption risks by data-driven optimization, simulation, and visibility. In *Handbook of Ripple Effects in the Supply Chain*; Springer: Cham, Switzerland, 2019; pp. 309–332.
17. Olivares-Aguila, J.; ElMaraghy, W. System dynamics modelling for supply chain disruptions. *Int. J. Prod. Res.* **2021**, *59*, 1757–1775. [[CrossRef](#)]
18. Zhang, Y.; Lam, J.S.L. Estimating economic losses of industry clusters due to port disruptions. *Transp. Res. Part A Policy Pract.* **2016**, *91*, 17–33. [[CrossRef](#)]
19. Cuong, T.N.; Kim, H.S.; You, S.S.; Nguyen, D.A. Seaport throughput forecasting and post COVID-19 recovery policy by using effective decision-making strategy: A case study of Vietnam ports. *Comput. Ind. Eng.* **2022**, *168*, 108102. [[CrossRef](#)]
20. Rogerson, S.; Svanberg, M.; Santén, V. Supply chain disruptions: Flexibility measures when encountering capacity problems in a port conflict. *Int. J. Logist. Manag.* **2022**, *33*, 567–589. [[CrossRef](#)]
21. Bai, X.; Jia, H.; Xu, M. Identifying port congestion and evaluating its impact on maritime logistics. *Marit. Policy Manag.* **2022**, *49*, 1–18. [[CrossRef](#)]
22. John, S.; Naim, M.M.; Towill, D.R. Dynamic analysis of a WIP compensated decision support system. *Int. J. Manuf. Syst. Des.* **2021**, *1*, 283–297.
23. Alkaabneh, F.M.; Lee, J.; Gómez, M.I.; Gao, H.O. A systems approach to carbon policy for fruit supply chains: Carbon tax, technology innovation, or land sparing? *Sci. Total Environ.* **2021**, *767*, 144211. [[CrossRef](#)]
24. Papanagnou, C.I. Measuring and eliminating the bullwhip in closed loop supply chains using control theory and Internet of Things. *Ann. Oper. Res.* **2022**, *310*, 153–170. [[CrossRef](#)]
25. Cuong, T.N.; Kim, H.S.; Nguyen, D.A.; You, S.S. Nonlinear analysis and active management of production-distribution in nonlinear supply chain model using sliding mode control theory. *Appl. Math. Model.* **2021**, *97*, 418–437. [[CrossRef](#)]
26. Alkaabneh, F.; Diabat, A.; Gao, H.O. A unified framework for efficient, effective, and fair resource allocation by food banks using an approximate dynamic programming approach. *Omega* **2021**, *100*, 102300. [[CrossRef](#)]
27. Khamseh, A.; Teimoury, E.; Shahanaghi, K. A new dynamic optimisation model for operational supply chain recovery. *Int. J. Prod. Res.* **2021**, *59*, 7441–7456. [[CrossRef](#)]
28. Fu, D.; Zhang, H.T.; Dutta, A.; Chen, G. A cooperative distributed model predictive control approach to supply chain management. *IEEE Trans. Syst. Man Cybern. Syst.* **2019**, *50*, 4894–4904. [[CrossRef](#)]
29. Alkaabneh, F.; Diabat, A. A multi-objective home healthcare delivery model and its solution using a branch-and-price algorithm and a two-stage meta-heuristic algorithm. *Transp. Res. Part C: Emerg. Technol.* **2022**, *147*, 103838. [[CrossRef](#)]
30. Yan, L.; Liu, J.; Xu, F.; Teo, K.L.; Lai, M. Control and synchronization of hyperchaos in digital manufacturing supply chain. *Appl. Math. Comput.* **2021**, *391*, 125646. [[CrossRef](#)]
31. Xu, X.; Kim, H.S.; You, S.S.; Lee, S.D. Active management strategy for supply chain system using nonlinear control synthesis. *Int. J. Dyn. Control* **2022**, *10*, 1981–1995. [[CrossRef](#)]
32. Cohen, M.; Cui, S.; Doetsch, S.; Ernst, R.; Huchzermeier, A.; Kouvelis, P.; Lee, H.; Matsuo, H.; Tsay, A.A. Bespoke supply-chain resilience: The gap between theory and practice. *J. Oper. Manag.* **2022**, *68*, 515–531. [[CrossRef](#)]
33. Moosavi, J.; Hosseini, S. Simulation-based assessment of supply chain resilience with consideration of recovery strategies in the COVID-19 pandemic context. *Comput. Ind. Eng.* **2021**, *160*, 107593. [[CrossRef](#)]
34. Mao, X.; Lou, X.; Yuan, C.; Zhou, J. Resilience-based restoration model for supply chain networks. *Mathematics* **2020**, *8*, 163. [[CrossRef](#)]
35. Rajesh, R. Network design for resilience in supply chains using novel crazy elitist TLBO. *Neural Comput. Appl.* **2020**, *32*, 7421–7437. [[CrossRef](#)]
36. Chen, H.; Cullinane, K.; Liu, N. Developing a model for measuring the resilience of a port-hinterland container transportation network. *Transp. Res. Part E Logist. Transp. Rev.* **2017**, *97*, 282–301. [[CrossRef](#)]
37. Rajesh, R. A fuzzy approach to analyzing the level of resilience in manufacturing supply chains. *Sustain. Prod. Consum.* **2019**, *18*, 224–236. [[CrossRef](#)]
38. Ramezankhani, M.J.; Torabi, S.A.; Vahidi, F. Supply chain performance measurement and evaluation: A mixed sustainability and resilience approach. *Comput. Ind. Eng.* **2018**, *126*, 531–548. [[CrossRef](#)]
39. Zhang, A.N.; Wagner, S.M.; Goh, M.; Asian, S. Quantifying supply chain disruption: A recovery time equivalent value at risk approach. *Int. J. Logist. Res. Appl.* **2021**, *24*, 1–21. [[CrossRef](#)]
40. Li, Y.; Zobel, C.W.; Seref, O.; Chatfield, D. Network characteristics and supply chain resilience under conditions of risk propagation. *Int. J. Prod. Econ.* **2020**, *223*, 107529. [[CrossRef](#)]
41. Gao, Y.; Leng, Y.; Shan, B. Control Supply Chain Risks in Digital Transformation: A New Way to Improve Supply Chain Resilience. *J. Organ. End User Comput.* **2022**, *34*, 1–18. [[CrossRef](#)]
42. Towill, D.R. Exponential smoothing of learning curve data. *Int. J. Prod. Res.* **1977**, *15*, 1–15. [[CrossRef](#)]
43. Wikner, J. Dynamic analysis of a production-inventory model. *Kybernetes* **2005**, *37*, 803–823. [[CrossRef](#)]
44. Xu, B.; Li, J.; Yang, Y.; Wu, H.; Postolache, O. Model and resilience analysis for handling chain systems in container ports. *Complexity* **2019**, *2019*, 9812651. [[CrossRef](#)]

45. Spiegler, V.L.; Naim, M.M.; Wikner, J. A control engineering approach to the assessment of supply chain resilience. *Int. J. Prod. Res.* **2012**, *50*, 6162–6187. [[CrossRef](#)]
46. Al-Khazraji, H.; Cole, C.; Guo, W. Optimization and simulation of dynamic performance of production–inventory systems with multivariable controls. *Mathematics* **2021**, *9*, 568. [[CrossRef](#)]
47. Disney, S.M.; Towill, D.R. A procedure for the optimization of the dynamics response of a vendor managed inventory system. *Comput. Ind. Eng.* **2002**, *43*, 27–58. [[CrossRef](#)]
48. Kristianto, Y.; Helo, P.; Jiao, J.R.; Sandhu, M. Adaptive fuzzy vendor managed inventory control for mitigating the Bullwhip effect in supply chains. *Eur. J. Oper. Res.* **2012**, *216*, 346–355. [[CrossRef](#)]
49. Disney, S.M.; Naim, M.M.; Towill, D.R. Genetic algorithm optimization of a class of inventory control systems. *Int. J. Prod. Econ.* **2000**, *68*, 259–278. [[CrossRef](#)]
50. Bešković, B.; Zanne, M.; Golnar, M. Dynamic Changes in Port Logistics Caused by the COVID-19 Pandemic. *J. Mar. Sci. Eng.* **2022**, *10*, 1473. [[CrossRef](#)]
51. Verschuur, J.; Koks, E.E.; Hall, J.W. Port disruptions due to natural disasters: Insights into port and logistics resilience. *Transp. Res. Part D Transp. Environ.* **2020**, *85*, 102393. [[CrossRef](#)]
52. Rožić, T.; Naletina, D.; Zajač, M. Volatile freight rates in maritime container industry in times of crises. *Appl. Sci.* **2022**, *12*, 8452. [[CrossRef](#)]

**Disclaimer/Publisher’s Note:** The statements, opinions and data contained in all publications are solely those of the individual author(s) and contributor(s) and not of MDPI and/or the editor(s). MDPI and/or the editor(s) disclaim responsibility for any injury to people or property resulting from any ideas, methods, instructions or products referred to in the content.